Exposure and Health
https://doi.org/10.1007/s12403-023-00534-3

ORIGINAL PAPER

Integrated Insights into Source Apportionment and Source-Specific Health Risks of Potential Pollutants in Urban Park Soils on the Karst Plateau, SW China

Longchao Liang[1,2] · Yaru Zhu[3] · Xiaohang Xu[4,2] · Wanbin Hao[1] · Jialiang Han[2] · Zhuo Chen[1] · Xian Dong[1] · Guangle Qiu[2]

Received: 21 September 2022 / Revised: 10 November 2022 / Accepted: 2 January 2023

Abstract

Polycyclic aromatic hydrocarbons (PAHs) and heavy metal(loid)s (HMs) pose risks to environmental and human health. Identification of priority control contaminants is important in guiding the management and control of these synchronous pollutants. A total of 247 soil samples were collected from 64 urban parks in the karst plateau city of Guiyang in SW China to determine the concentrations, spatial distributions, and health risks of PAHs and HMs. The results indicate that dibenz(ah) anthracene and benzo(a)pyrene are the main PAHs species of high ecological risk, and Cr, Mn, and Ni pose elevated ecological risk among the HMs. Four sources were identified for PAHs (biomass burning, coke oven, traffic sources, and coal burning) and HMs (traffic sources, coal burning, industrial sources, and natural sources). The non-carcinogenic risk (NCR) and total carcinogenic risk (TCR) of PAHs were all determined to be negligible and at acceptable levels, several orders of magnitude below those of HMs. The NCR and TCR values of HMs were relatively high, especially for children (11.9% of NCR > 1; 79.1% of TCR > 10^{-4}). Coal burning and natural sources make the greatest contributions to the NCR and TCR values from karst park soils in Guiyang. Considering HMs bioavailability, NCR and TCR values were rather low, due to the high residual HM fractions. Integrated insights into source specific ecological and human health risk indicate future directions for management and control of synchronous PAH and HM pollution, particularly for karst plateau areas.

Keywords Soil pollution · Monte Carlo simulation · Positive matrix factorization · Priority factors · Sequential extraction

Introduction

Urban areas, with their dense populations, contain > 50% of the world's population and 3% of the global land surface area (Edmondson et al. 2012; Li et al. 2018). Rapid urbanization and industrialization over recent decades have accelerated the discharge of anthropogenic pollutants to the environment (Sun et al. 2020), particularly in developing countries (Zhou et al. 2004). Overcrowded urban areas are exposed to significant loadings of polycyclic aromatic hydrocarbons (PAHs) and heavy metal(loid)s (HMs), making such environments a global public-health issue.

Both PAHs and HMs are of increasing concern in urban soils (Huang et al. 2021; Peng et al. 2013), where their accumulation has detrimental effects on plant growth and results in secondary pollution of water systems (Zhang et al. 2019a). Local populations are exposed to risk through ingestion, inhalation, and dermal contact of HMs and PAHs (Ciarkowska et al. 2021), with chronic exposure leading to accumulation in various tissues and organs that may cause long-term damage to nervous, endocrine, and immune systems, as well as effects on metabolism (Kim et al. 2013; Mallah et al. 2022). An understanding of synchronous PAHs

✉ Xiaohang Xu
xxh1119@foxmail.com; xuxh@gzu.edu.cn

1 School of Chemistry and Materials Science, Guizhou Normal University, Guiyang 550025, China

2 State Key Laboratory of Environmental Geochemistry, Institute of Geochemistry, Chinese Academy of Sciences, Guiyang 550081, China

3 College of Resource & Environment, Henan Agricultural University, Zhengzhou 450002, China

4 Key Laboratory of Karst Georesources and Environment, Ministry of Education, College of Resources and Environmental Engineering, Guizhou University, Guiyang 550025, China

Published online: 07 January 2023

and HMs contamination in urban soil is therefore of particular significance.

Once released into the environment, particulate pollutants are deposited on surface soil, from which they may be re-suspended, making soil both a pollution sink and source (Jiang et al. 2016). Urban soils play a major role in stabilizing urban environments, with urban parks being particularly important in the leisure activities of residents and in regulating urban ecosystems (Huang et al. 2021). Users are inevitably exposed to deposited PAHs and HMs by direct contact with park soils.

Health risk evaluation is an effective tool for identifying priority-control pollutants in different environment media including soils, groundwater, and foodstuffs (Han et al. 2022; Liu et al. 2022; Wang et al. 2022; Wei et al. 2022; Xu et al. 2020). Most evaluations to date have involved deterministic models with fixed parameters (Brtnický et al. 2019), with uncertainties leading to biased results (Sun et al. 2022). Traditional risk evaluation methods have been based on conservative "reasonable" risk exposure, which is difficult to quantify, with weaknesses arising through the use of fixed parameters or mean input data. More recently, a series of methods, including Monte Carlo simulations (MCs) and Bayesian analysis have been introduced in health risk evaluations to overcome such uncertainties (Islam et al. 2019; Jiménez-Oyola et al. 2021).

Although concerns about contamination of urban park soils is increasing, previous studies have focused mainly on contamination by single HMs or PAHs (Khan et al. 2016; Liu et al. 2022; Vega et al. 2022), and few have considered the combined effects of multiple contaminants (Wu et al. 2019). In this study, MCs were applied together with positive matrix factorization (PMF) modeling in health risk evaluation to improve our understanding of source-based non-carcinogenic risk (NCR) and total carcinogenic risk (TCR) due to urban park soils.

The avoidance of further soil PAHs and HMs pollution and associated health risks requires an understanding of pollution sources and their contribution rates. Receptor models are widely used in identifying pollution sources for surface-soil and groundwater systems (Guan et al. 2018; Li et al. 2021; Liu et al. 2022). PMF modeling, as recommended by the US Environmental Protection Agency (USEPA), has been successfully employed in PAH and HM source identification for different environment media, with weighting of the uncertainties in initial data and non-negative results (Sun et al. 2020; Zhang et al. 2021). To improve result credibility, PMF is often combined with multivariate analyses such as Pearson correlation analysis.

Guiyang, a karst plateau city in the eastern Yunnan-Guizhou Plateau, SW China, was selected as the study area and is characterized by rugged and hilly topography. Soils in karst regions generally have high HM backgrounds (Zhan et al. 2021). Most of Guiyang lies in an inter-mountain basin, which blocks the atmospheric dispersion of pollutants. Tourism is a principle economic industry, contributing ~ 38.7% of the local gross domestic product (GSY 2021). Even during the COVID-19 pandemic period, urban parks in Guiyang received 152 million visitors during 2021. Previous studies have shown the elevated HM levels in farmland soils and soils from industrial sites around Guiyang (Cai et al. 2021; Cui et al. 2022; Xuan et al. 2018). However, little is known about HM pollution sources in park soils, and even less about the effects of the combined PAH and HM contamination. Special attention is required to fill this knowledge gap.

The objectives of this study were to (1) determine PAH and HM contamination characteristics in karst park soils; (2) identify the sources of PAH and HM pollution; (3) evaluate the combined human health risks of PAHs and HMs; and (4) establish priority control factors through the understanding of relationships between HMs, pollution sources, and health risks associated with urban park soils. The findings of the study will provide vital information for policy-makers for the development of measures targeting exposure.

Methods

Study Area

Guiyang (106° 07′–107° 17′E, 26° 11′–27° 22′N) lies on the eastern slope of the Yunnan–Guizhou Plateau, in an extensive and well-developed karst area (Peng & Deng 2020). The karst geomorphology makes it an environmentally fragile ecological environment. Karst areas in Guiyang total ~ 6800 km^2, or 85% of total area. Rocky desertification areas make up ~ 51% of the total area, and soil erosion is severe. The Guiyang climate is dominated by a subtropical monsoon season, with a mean annual temperature of 14.9 °C and precipitation of 1378 mm (GSY 2021). Industry was the pillar of the Guiyang economy, including coal-fired power plants, non-ferrous metal smelting, further processing, and cement production (Xu et al. 2016). Guiyang is rich in coal resources, and coal is widely used by local residents.

Sampling and Processing

A total of 247 soil samples (0–15 cm) were collected from 64 parks across Guiyang during September–October, 2021, including the Guanshanhu, Baiyun, Wudang, Huaxi, Yunyan, and Nanming districts (Fig. 1). Each sample of ~ 500 g included three sub-samples. Samples were collected using stainless shovels and placed in labeled sterile polythene bags. After removal of impurities, samples were air-dried, mixed thoroughly, and ground by mortar and pestle to pass through a 200-mesh sieve.

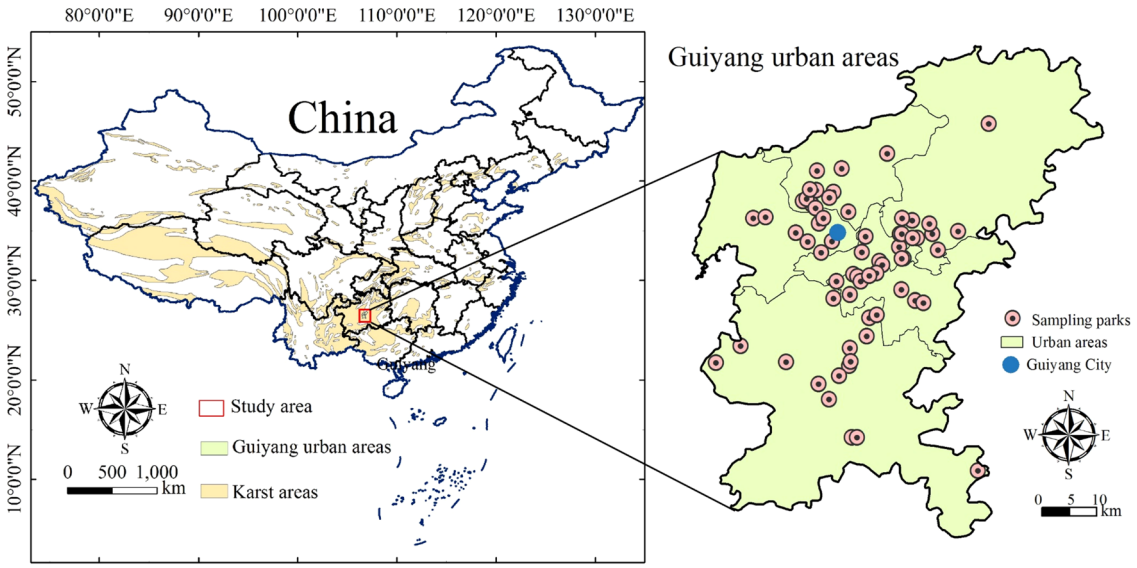

Fig. 1 Sampling sites in urban parks in the karst plateau city, Guiyang

HMs Analysis

Soil samples were prepared for analysis as follows (Han et al. 2022). Each sample (~0.05 g) was weighed into a Teflon-lined stainless-steel bomb and digested with ultrapure 3 mL HNO_3 (15.8 M) and 0.5 mL HF (23 M) at 160 °C for 48 h. After cooling, the solution was evaporated to near-dryness and ultrapure water (4 mL) and HNO_3 (1 mL) were added before further at 160 °C for 16 h.

Four HM fractions were obtained by the sequential extraction method proposed by The European Community Bureau of Reference (BCR) (Beane et al. 2016): Fraction 1, acid-soluble fraction; Fraction 2, reducible fraction; Fraction 3, oxidizable fraction; and Fraction 4, residual fraction.

Nickel, Cr, Cu, As, Pb, Sb, Zn, Cd, and Mn concentrations were determined by inductively coupled plasma–mass spectrometry (ICP–MS, Agilent Technologies 7700, USA), using an Rh internal standard. Soil reference materials (GBW07405, Geophysical and Geochemical Prospecting Institute, Chinese Academy of Geological Sciences, China), duplicates, and reagent blanks were also analyzed.

PAHs Analysis

For PAH analysis, soil samples (~5 g) were extracted twice by solvent extraction (ASE350, Dionex) at 100 °C and 10 MPa with a 5 min static cycle, using acetone and n-hexane (1:1, v/v). The extract was evaporated in a rotary evaporator, concentrated, and the solvent changed to n-hexane. Concentrated extracts were purified using silica gel columns, with PAHs being eluted using a mixture of dichloro-methane and n-hexane (3:7, v/v). The mixed solvent was again concentrated and the residue dissolved in n-hexane for analysis by ultra-performance liquid chromatography (ACQUITY H-Class, Waters, USA) (Fan et al. 2019).

Sixteen USEPA priority PAHs (Σ_{16}PAHs) were also analyzed: naphthalene (Nap), acenaphthylene (Acy), acenaphthene (Ace), fluorene (Flu), phenanthrene (Phe), anthracene (Ant), fluoranthene (Fla), pyrene (Pyr), benzo(a)anthracene (BaA), chrysene (CHR), benzo(b)fluoranthene (BbF), benzo(k)fluoranthene (BkF), benzo(a)pyrene (BaP), dibenz(ah)anthracene (DBA), indeno(1,2,3-cd)pyrene (InP), and benzo(ghi)perylene (BghiP).

PMF Model

As a receptor model, PMF is typically used to qualitatively apportion pollutant sources in both soil and water environments. PMF v. 5.0 resolves sampling data into two matrices: the factor contribution matrix and factor distribution matrix. Factors were obtained using Eq. (1) (Guan et al. 2019):

$$x_{ij} = \sum_{k=1}^{p} g_{ik} f_{kj} + e_{ij} \quad (1)$$

where x_{ij} indicates the concentration of the HMs, i is the number of samples, j denotes the chemical species, p is the number of sources, e is the error for each sample, and u is the uncertainty, calculated as follows:

$$\text{For} x_{ij} \le \text{MDL}, u_{ij} = \frac{5}{6} \times \text{MDL} \quad (2)$$

$$\text{For} x_{ij} > \text{MDL}, u_{ij} = \sqrt{(\sigma \times x_{ij})^2 + (0.5 \times \text{MDL})^2} \quad (3)$$

where MDL is the detection limit for each element, and σ is relative standard deviation.

Pollution Characteristics

To determine the level of contamination by a single element or compound, pollution indices (P_i, Eq. 4) of PAHs and HMs were adopted for some individual PAHs (DBA, BaP, BaA, BkF, BbF, InP, Nap, and CHR) and all studied HMs (Cr, Mn, Ni, Cu, Zn, As, Cd, Sb, and Pb), as background levels were available for these compounds (Table S1).

$$P_i = C_i / B_i \tag{4}$$

where C_i is the concentration of PAH_i (ng g^{-1}) or HM_i (mg kg^{-1}) in soil sample, and B_i is corresponding background value.

Ecological Risk Model Based on PMF

To quantitatively assess potential ecological risks (PER) from different sources of PAHs or HMs, a combination of PMF, and PER or toxic equivalent concentration (TEQ) was applied (Huang et al. 2022) with processing as follows:

$$* C_{jk}^{i} = n\% \times C_{jk} \tag{5}$$

where $* C_{jk}^{i}$ is the mass contribution of HM k from source i for sample j; n% denotes the ratio of HM k in sample j from different sources; and C_{jk} is the original concentration of HM k in the sample j.

Toxic equivalency factors (TEFs) were calculated to quantify the carcinogenic and toxic potency of individual PAHs relative to BaP and the total quantity of PAHs (ΣPAHs TEQ) (Zhang et al. 2019b). The TEQ was obtained through Eq. (6):

$$TEQ = \sum (* C_{jk}^{i} \times TEF_i) \tag{6}$$

where TEF_i is the corresponding TEF (Table S1). The ecosystem potential ecological risk index (RI) of HMs was estimated using Eq. (7) (Huang et al. 2022).

$$(* E_r^i)_{jk}^{i} = T_r^i * C_{jk}^{i} / C_b^i \tag{7}$$

$$RI = \sum_{i=1}^{n} (* E_r^i)_{jk}^{i} \tag{8}$$

where E_r^i represents the single ecological risk index for HM i; and T_r^i denotes the toxic response coefficient of that HM. Values of T_r^i for As, Cd, Cr, Cu, Mn, Ni, Pb, Sb, and Zn were 10, 30, 2, 5, 1, 5, 5, 40, and 1, respectively (Hakanson 1980; Jiang et al. 2020).

Risk Assessments

Three primary exposure pathways (ingestion, dermal contact, and inhalation) for soil pollutants were considered. Human NCR and TCR were evaluated by MCs with Crystal Ball 11.1.24 software © (Oracle,

Redwood City, CA, USA) software using the following equations, with all the related parameters are given in Table S2–S4 (Han et al. 2022). To ensure the reliability of results, 10,000 iterations were performed.

$$* ADD_{jk_{ingestion}}^{i} = \frac{* C_{jk}^{i} \times IR_S \times EF \times ED}{BW \times AT \times 10^6} \tag{9}$$

$$* ADD_{jk_{dermal}}^{i} = \frac{* C_{jk}^{i} \times SA \times SL \times ABF \times EF \times ED}{BW \times AT \times 10^6} \tag{10}$$

$$* ADD_{jk_{inhal}}^{i} = \frac{* C_{jk}^{i} \times IR_a \times EF \times ED}{BW \times AT \times PEF} \tag{11}$$

$$HI = \sum HQ_{jk}^{i} = \sum \frac{* ADD_{jk_1}^{i}}{RfD_i} \tag{12}$$

$$TCR = \sum CR = \sum * ADD_{jk_1}^{i} \times SF_i \tag{13}$$

where $* ADD_{jk_{ingestion}}^{i}$, $* ADD_{jk_{dermal}}^{i}$, $* ADD_{jk_{inhal}}^{i}$ are the average daily intake dose of HM or PAH i in sample j through ingestion, dermal contact, and inhalation contact, respectively, and HQ is the average hazard quotient. The sum of one category of HQ is the hazard index (HI).

The incremental lifetime cancer risk (ILCR) model was used to evaluate the carcinogenic risk from ingestion, dermal contact, or inhalation of PAHs (Ambade et al. 2022; Ma et al. 2021). An ILCR $< 10^{-6}$ indicates no significant carcinogenic risk, $10^{-6} <$ ILCR $< 10^{-4}$ indicates acceptable carcinogenic risk, ILCR $> 10^{-4}$ indicates unacceptable carcinogenic risk from PAHs (Chen et al. 2022).

$$* ILCR_{jk_{ingestion}}^{i} = \frac{* C_{jk}^{i} \times TEF_i \times CSF_{ingestion} \times \sqrt[3]{BW/70} \times IR_s \times EF \times ED}{BW \times AT \times 10^6} \tag{14}$$

$$* ILCR_{jk_{dermal}}^{i} = \frac{* C_{jk}^{i} \times TEF_i \times CSF_{dermal} \times \sqrt[3]{BW/70} \times SA \times SL \times ABF \times EF \times ED}{BW \times AT \times 10^6} \tag{15}$$

$$* \mathrm{ILCR}^{i}_{jk_{inhal}} = \frac{* C^{i}_{jk} \times \mathrm{TEF}_{i} \times \mathrm{CSF}_{inhal} \times \sqrt[3]{\mathrm{BW}/70} \times \mathrm{IR}_{a} \times \mathrm{EF} \times \mathrm{ED}}{\mathrm{BW} \times \mathrm{AT} \times \mathrm{PEF}} \quad (16)$$

$$\mathrm{TCR} = * \mathrm{ILCR}^{i}_{jk_{ingestion}} + * \mathrm{ILCR}^{i}_{jk_{dermal}} + * \mathrm{ILCR}^{i}_{jk_{inhal}} \quad (17)$$

where IR_s and IR_a are the soil ingestion and inhalation rates, EF is exposure frequency, ED exposure duration, BW body weight, SA skin surface area, SL skin adherence factor, ABF dermal absorption factor, SF carcinogenic slope factor for HMs, and CSF is the carcinogenic slope factor of Bap. All parameters are listed in Tables S2–S4.

Statistical Analysis

All statistical calculations involved Microsoft™ EXCEL 2016. The locations of sampling sites and the spatial distributions of pollutants were obtained using ArcGIS 10.4. All other figures were prepared using ORIGIN 2021 software. The Kolmogorov–Smirnov (K–S) test of initial and log-transformed concentrations was applied to check distributions. If data were normally distributed, the arithmetical mean value was more representative; for log-normal data distributions, the geometric mean value was more representative; and where distributions were skewed, the median value was more representative.

Results and Discussion

PAHs and HMs in Park Soils

Overall, after K–S testing, the concentrations of Σ_{16}PAH and some individual PAHs (Nap, Ace, Flu, Fla, Pyr, BaA, Bap, DBA, InP, and BghiP) in karst park soils displayed a skewed distribution (Table 1). For the remaining PAHs, Acy, Phe, Ant, CHR, and BkF followed a lognormal distribution, and BbF a normal distribution. High PAH concentrations were observed in the Baiyun, Huaxi, and Yunyan districts (Fig. S1), which were industrial and old urban areas. The PAHs followed the decreasing concentration order BbF > Phe > BkF > Nap > Ace > BaA > Ant > BghiP > CHR = Bap > DBA > Pyr > InP > Acy > Flu > Fla. Σ_{16}PAH concentrations ranged from 142 to 7223 ng g^{-1} with a median value of 434 ng g^{-1}, consistent with or slightly higher than those reported in park soils in Malopolska (Poland), and Guangzhou and Beijing (China), and substantially lower than those in Miami and Milwaukee (USA), Nanjing, Shanghai, Xiamen, Urumqi, Xi'an, Lanzhou, and Hong Kong (China) (Table 2); and the reported average Σ_{16}PAH concentration in urban soils in China (Yu et al. 2019). The relatively low Σ_{16}PAH concentrations in park soils may be due to a lack of pollution sources, including lower vehicular emissions and less intensified commercial districts in Guiyang.

Concentrations of low-molecular-weight (LMW) 2–3 ring PAHs and high-molecular-weight (HMW) 4–6 ring PAHs were 136 and 287 ng g^{-1}, respectively; HMW PAHs thus accounted for most of the PAHs in park soils (Fig. S2, Table 2). The high contribution of HMW PAHs may be due to high-temperature processes such as combustion of fuels in vehicle engines (Mostert et al. 2010). HMW PAHs can persist for longer periods with lower rates of degradation than LMW PAHs so (Wang et al. 2011), despite the lower Σ_{16}PAH concentration, the high levels of HMW PAHs require special attention.

The concentrations of most HMs (Ni, Cr, As, Sb, Zn, Cd, and Mn) in park soils were lognormally distributed, whereas, Cu and Pb followed normal and skewed distributions, respectively. Overall, the concentrations of Cu, As, Zn, and Cd were higher than those recorded previously in farmland in Guiyang (Cai et al. 2021). Except for Cd, the concentrations of all HMs were greater than those of Guizhou geochemical baselines (CNEMC 1990), implying HM accumulation in park soils. The highest concentrations recorded for Cr (363 mg kg^{-1}), Pb (1045 mg kg^{-1}), and Cd (4.19 mg kg^{-1}) were higher than values reported previously for Guanshanhu district, Guiyang, whereas, that of As (139 mg kg^{-1}) was consistent with previous values (Cui et al. 2022). The coefficients of variation (CVs) of all HMs ranged from 42.2 to 201%, indicating moderate to strong variation. The high concentrations and CVs of Pb, As, Sb, Cd, and Mn suggest they originate from anthropogenic sources (Zhuo et al. 2020). Elevated concentrations were generally observed in and around urban centers, with HM hotspots in the southern part of the city (Fig. S3). Most HMs were thus highly impacted by human activities. Furthermore, most recorded Ni, Cr, Cu, As, Mn, Zn, and Cd concentrations were higher than those of parks soils worldwide (Table 2), possibly due to high geologic backgrounds in such in karst areas (Kong et al. 2018). The element generally typical of traffic sources, Pb had generally lower concentrations than those in park soils worldwide, indicating relatively low emissions (Bineshpour et al. 2021).

Source Identification for PAHs and HMs in Park Soils

To achieve convincing and quantifiable source identification, diagnostic ratios, correlation analysis, and PMF receptor modeling were used for PAHs, and correlation analysis and PMF modeling for HMs. To verify source apportionments, correlations between PMF factor contributions and concentrations of PAHs or HMs were also investigated (Huang et al. 2021). In PMF processing, four factors for both PAHs and HMs were determined after comparing robust and true Q values (Fig. 2a, d) (Kwon & Choi 2014).

Table 1 Concentrations of PAHs and HMs in park soils in Guiyang

Categories	Element	Arithmetic Mean	Geometric mean	Median	Standard deviation	Variation coefficient (%)	Skewness	Kurtosis	Range	Minimum	Maximum	Distribution
PAHs (ng/g)	Nap	33.7	27.0	**21.5**	28.4	84.5	2.55	7.00	141	9.93	151	Skewed
	Ace	35.0	24.0	**20.5**	42.1	120	2.90	8.25	195	6.84	201	Skewed
	Flu	47.4	15.4	**8.93**	71.7	151	1.53	0.823	239	2.40	242	Skewed
	Acy	16.6	**11.8**	9.97	18.4	111	3.57	16.6	117	3.81	121	Lognormal
	Phe	97.2	**35.6**	28.1	285	293	7.01	52.8	2236	4.64	2241	Lognormal
	Ant	29.4	**19.5**	18.2	49.2	168	6.66	49.4	390	3.77	394	Lognormal
	Fla	26.3	5.41	**4.55**	131	499	7.73	60.7	1043	0.390	1044	Skewed
	Pyr	66.0	19.7	**15.8**	124	188	3.14	10.8	668	2.22	671	Skewed
	BaA	63.6	27.3	**19.7**	107	169	3.52	15.6	663	1.81	665	Skewed
	CHR	32.3	**18.4**	16.3	54.4	168	5.19	32.8	392	4.74	397	Lognormal
	BbF	**50.8**	39.4	46.3	35.5	69.9	1.42	2.94	186	3.73	189	Normal
	BkF	56.5	**26.1**	26.4	186	329	7.73	61.1	1501	5.36	1506	Lognormal
	Bap	31.7	23.0	**18.4**	50.0	158	6.67	49.3	392	9.33	401	Skewed
	DBA	58.0	25.2	**16.3**	165	284	7.16	54.5	1298	7.35	1306	Skewed
	InP	23.0	15.9	**12.5**	35.6	155	6.11	43.0	273	4.84	278	Skewed
	BghiP	38.2	23.4	**18.8**	75.8	199	6.50	46.7	588	2.83	591	Skewed
	PAHs	705	465	**434**	1018	144	4.88	28.2	7081	142	7223	Skewed
	LMW	259	165	136	369	142	4.60	26.0	2539	47.2	2586	Skewed
	HMW	446	287	255	752	169	6.13	43.1	5760	77.2	5837	Lognormal
HMs (mg/kg)	Ni	62.6	**53.5**	51.1	35.3	56.3	0.910	0.174	146	14.2	160	Lognormal
	Cr	111	**103**	106	46.7	42.2	2.73	13.2	321	42.6	363	Lognormal
	Cu	**64.1**	52.2	57.0.0	36.8	57.4	0.668	0.0160	159	4.05	163	Normal
	As	41.2	**33.1**	31.7	31.1	75.5	1.84	2.98	132	6.53	139	Lognormal
	Pb	63.4	44.8	**40.0**	128	201	7.47	58.0	1028	16.7	1045	Skewed
	Sb	3.13	**2.49**	2.50	2.90	92.6	4.22	23.4	20.6	0.470	21.1	Lognormal
	Zn	171	**154**	152	87.9	51.4	1.93	4.95	457	59.2	516	Lognormal
	Cd	0.705	**0.564**	0.525	0.661	93.8	3.59	14.9	4.05	0.140	4.19	Lognormal
	Mn	848	**700**	729	527	62.1	1.53	2.92	2739	71.5	2810	Lognormal

The data in bold are more representative of the corresponding concentrations

Table 2 PAHs and HMs in park soils worldwide

City	As (mg/kg)	Cd (mg/kg)	Cr (mg/kg)	Cu (mg/kg)	Mn (mg/kg)	Ni (mg/kg)	Pb (mg/kg)	Zn (mg/kg)	PAHs (ng/g)	References
Malopolska, Poland	–	1.74 ± 1.15	–	–	–	–	31.2 ± 10.4	176 ± 55.2	366 ± 118	Ciarkowska et al. (2019)
Miami, USA									1600	Banger et al. (2010)
Zielona Góra Poland	–	–	–	35.8 ± 65.7	–	–	41.8 ± 60.6	92.1 ± 72.8	–	Greinert (2015)
Milwaukee, USA	–	–	–	–	–	–	–	–	7869	Siemering & Thiboldeaux (2021)
Aberdeen, Scotland	–	–	23.9 ± 2.30	27.0 ± 64.0	286 ± 52.0	14.9 ± 1.60	94.4 ± 216	58.4 ± 7.60	–	Paterson et al. (1996)
Madrid, Spain	–	–	16.9 ± 10.2	36.6 ± 31.5	423 ± 89.4	9.02 ± 4.42	102 ± 136	139 ± 62.7		Izquierdo et al. (2015)
Malayer, Iran	0.500	–	–	11.5	–	–	10.7	82.7		Solgi & Oshvandi (2018)
Krakow, Poland	–	0.8 ± 0.69	16.3 ± 3.30	55.5 ± 20.3	–	10.5 ± 1.60	120.2 ± 60.3	177 ± 126	–	Gasiorek et al. (2017)
Brno, Czech Republic	–	0.276 ± 0.183	-	16.6 ± 7.60	–	–	27.2 ± 14.2	59.0 ± 34.5	–	Brtnický et al. (2019)
Copiapó,Chile				361	947		31	114		Vega et al. (2022)
La Serna-Coquimbo, Chile				80	660		24	< 103		Vega et al. (2022)
Gran Santiago, Chile				191	1119		48	179		Vega et al. (2022)
Nanjing, China	12.1	0.120	72.4	40.1		34.2	66.0	105	2371	Wang et al. (2020)
Shanghai, China	17.7 ± 5.22	0.362 ± 0.125	0.362 ± 0.125	38.5 ± 15.4	–	35.4 ± 13.3	36.3 ± 16.0	144 ± 42.8	2230 ± 3690	Liang et al. (2019)
Beijing, China	12.0 ± 3.89	0.490 ± 0.110	63.6 ± 49.2	35.5 ± 13.3	–	27.1 ± 3.45	36.4 ± 14.6	146 ± 49.4	466 ± 6.00	Liu et al. (2020, 2021); Qu et al. (2020)
Guangzhou, China		0.220 ± 0.0400	58.4 ± 17.8	73.5 ± 22.1	–	28.2 ± 6.64	124 ± 47.4	98.3 ± 11.2	286 ± 193	Gu et al. (2016); Ke et al. (2017)
Xiamen, China	11.8	0.240	17.6	19.8	433	7.90	49.5	92.2	641	Lu et al. (2008); Zhao et al. (2020)
Urumqi, China	–	–	–	–	–	–	–	–	1815 ± 652	Chen et al. (2013)
Xi'an, China	–	–	–	–	–	–	–	–	629	Bao et al. (2018)
Lanzhou, China	–	–	–	–	–	–	–	–	521	Jiang et al. (2016)
Hong Kong, China	–	0.350 ± 0.0900	21.8 ± 6.70	6.37 ± 4.02	–	5.30 ± 2.00	39.6 ± 23.3	46.8 ± 21.5	812	Chung et al. (2007); Lee et al. (2006)

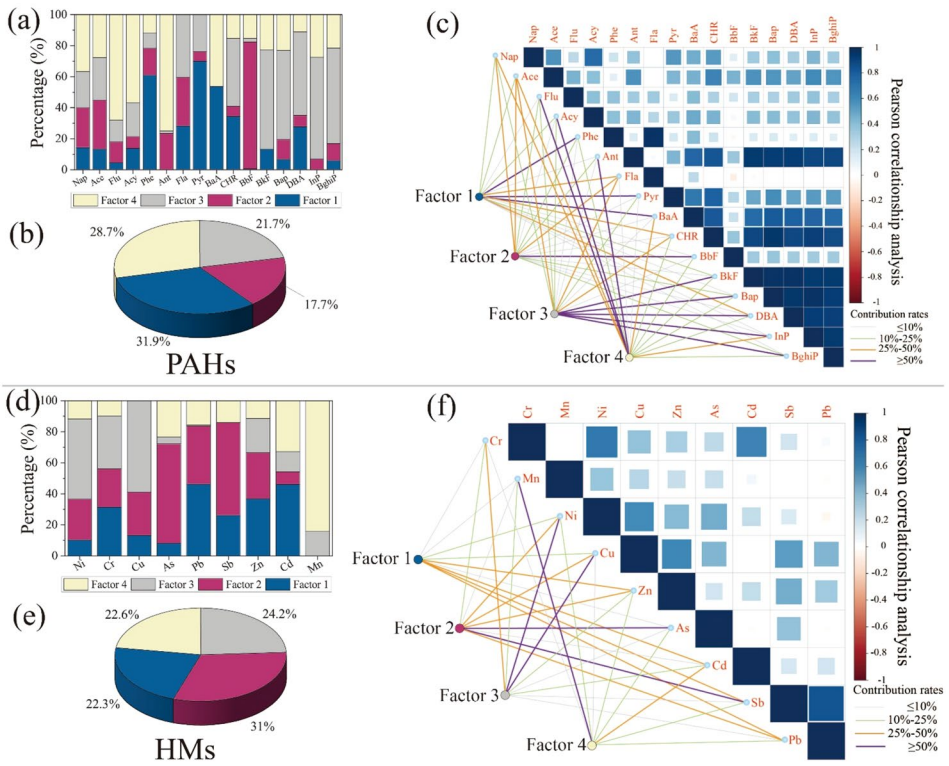

Fig. 2 Source apportionment of PAHs and HMs. **a**, **d** PMF factor profiles of PAHs and HMs; **b**, **e** percentage contributions of each PMF factor. **c**, **f** Pearson correlations among PAHs and HMs, and between PAHs, HMs, and PMF factors

PAHs

Diagnostic ratios are commonly applied in PAHs source identification (Fig. S4). PAH LMW/HMW ratios of < 1 indicate pyrogenic sources such as incomplete combustion of biomass or fossils fuels (Tobiszewski & Namieśnik 2012). Here, Flu/(Flu + Pyr) ratios were in the range of 0.0137–0.983; 53.1% of ratios were > 0.5, indicating fossil-fuel combustion (Ravindra et al. 2008). For Ant/(Ant + Phe) ratios, 87.5% were > 0.1 indicating pyrogenic sources including oil, coal, and biomass combustion (Pies et al. 2008). For BaA/(BaA + CHR) ratios 87.5% were > 0.5, again indicating biomass and coal combustion sources (Yunker et al. 2002). The mean Bap/BghiP ratio was 0.831, with 82.8% of the ratios being > 0.6, indicating traffic sources (Katsoyiannis et al. 2007). For InP/(InP + BghiP) ratios, 92.2% were in the range of 0.2–0.5, indicating petroleum combustion sources (Yunker et al. 2002). Preliminary analysis thus indicates that PAHs in karst park soils originate from various sources, with fossil-fuel, biomass, coal combustion, and traffic sources predominating.

Further quantitative classification of PAH sources involved the PMF receptor model. Factor 1, heavily loaded with Phe (60.9%), Pyr (69.9%), and BaA (53.7%), was significantly correlated with Phe, Pyr, and BaA concentrations (Fig. 2c). Phe and BaA were previously apportioned from wood/grass burning (Zheng et al. 2019); Phe and Pyr were identified as being sourced mainly from biomass combustion (Jiang et al. 2014). Factor 1 was therefore defined as biomass burning.

Factor 2 was characterized by BbF (81.7%), followed by Ace (31.6%) and Fla (31.4%), with the strongest relationship with BbF (Fig. 2c). Phe and Bap have loadings of 17.4 and 12.8%, respectively. BbF is an indicator of emissions from coke ovens (Yang et al. 2013), together with Fla and Phe (Simcik et al. 1999). Ace and Bap have also been reported as originating from coke production (Khalili et al. 1995). Factor 2 thus indicates coke-oven sources.

Factor 3 was loaded predominantly with Fla (40.5%), CHR (43.8%), BkF (63.9%), Bap (57.3%), DBA (53.9%), InP (65.5%), and BghiP (61.4%), with strong correlations with BkF, Bap, DBA, InP, and BghiP concentrations (Fig. 2c). These HMW PAHs are derived from high-temperature combustion sources, including diesel combustion (Simcik et al. 1999); CHR, DBA, InP, and BghiP represent diesel emissions (Cetin et al. 2017); DBA, BkF, and BghiP were identified as being due to petroleum combustion (Konstantinova et al. 2020). Factor 3 is thus considered to represent traffic sources.

Factor 4 had high loadings of Nap (36.5%), Flu (68%), Acy (56.9%), and Ant (75.0%), with strong correlation with Flu, Acy, and Ant concentrations (Fig. 2c). Nap is released during incomplete combustion (Simcik et al. 1999); Flu is typical of coal combustion (Jiang et al. 2021; Larsen & Baker 2003); and Acy was previously identified

as a coal-burning marker (Wang et al. 2015). Factor 4 thus represents coal burning.

The PMF modeling results thus indicated that biomass burning, coke ovens, traffic sources, and coal burning are primary sources of PAH contamination in park soils on the karst plateau. The average contributions of individual sources to Σ_{16}PAHs were 31.9% for Factor 1, 28.7% for Factor 4, 21.7% for Factor 3, and 17.7% for Factor 2.

HMs

For HMs, Factor 1 was heavily loaded with Pb (46.2%), Cd (46.0%), and Zn (36.7%). Previous studies have suggested that Pb and Zn are markers of vehicle emissions (Liu et al. 2021). Although the use of Pb in gasoline has been banned, engine wear and braking still discharge Pb and Cd (Jin et al. 2019). Tires and lubricants also contain Cd, and Zn is a component of tires, bitumen, hardeners, and exhaust emissions (Huang et al. 2021). These HMs are initially deposited near roads, and are resuspended to enter park soils (Dao et al. 2014). Factor 1 thus represents traffic sources.

Factor 2 was dominated by As (64.3%), Sb (59.8%), and Pb (37.5%), with strong correlation with As and Sb concentrations (Fig. 2f). Coal consumed in Guiyang is characterized by high As contents, and coal-borne arsenicosis has been reported in Guizhou (Wang et al. 2019a). Coal combustion also contributed to the increasing trend in Pb emissions during 1980–2008 (Tian et al. 2012). Factor 2 is thus attributed to coal burning.

Factor 3 was characterized mainly by Cu (58.8%) and Ni (51.7%), with strong correlations with Cu and Ni concentrations (Fig. 2f). The significant correlation ($r = 0.593$, $p = 0$) between Cu and Ni concentrations implies a common source (Han et al. 2022). Copper is attributed to industrial activities (Zhao et al. 2019), whereas Ni is typically used in alloys (Gu et al. 2014). Atmospheric deposition from industrial waste, and incineration of domestic waste could thus be sources of Cu (Huang et al. 2007). Therefore, Factor 3 is associated with industrial sources.

Factor 4 had a high Mn loading (84.3%), followed by Cd (32.9%) and As (23.4%) with strong correlation with Mn concentration ($r = 0.908$, $p = 0$). Manganese is commonly identified as arising from natural sources (Liang et al. 2017). The geometric mean of Mn was lower than the corresponding background values (CNEMC 1990). Manganese concentrations were closest to geochemical background values when soil HMs were dominated by parent material (Liang et al. 2017). Factor 4 thus represents natural sources.

Overall, anthropogenic activities, particularly coal burning (31.0%), are the primary sources of HMs in park soils. Reductions in coal burning are thus critical for reducing HM levels in park soils on the karst plateau.

Pollution Characteristics of PAHs and HMs

Pollution indices of PAHs were calculated using risk-screening values for soil contamination of developed land, and HM levels were calculated from their corresponding background values.

The pollution indices of PAHs followed the order DBA (1.05E–1) > BaP (5.76E–2) > BaA (1.16E–2) > BbF (9.24E–3) > InP (4.17E–3) > NaP (1.35E–3) > BkF (1.03E–3) > CHR (6.58E–5) (Fig. S5). Only 1.56% of the values DBA exceeded 1, indicating the limited degree of pollution by individual PAH species. The maximum P_i value of DBA was 2.37 times the relevant risk-screening value, but only 0.237 times the risk-intervention value, indicating the potential risk to residents. Furthermore, the following classification criteria were used for Σ_{16}PAH: Σ_{16}PAH < 200 ng g^{-1}, non-contaminated; 200–600 ng g^{-1}, weakly contaminated; 600–1000 ng g^{-1}, contaminated; and > 1000 ng g^{-1}, heavily contaminated, with recommended values being used (Maliszewska-Kordybach 1996). Using these criteria, Σ_{16}PAH in 12.5% (8/64) of karst parks were considered non-contaminated, 53.1% (34/64) weakly contaminated, 17.2% (11/64) contaminated, and 17.2% (11/64) heavily contaminated.

Pollution indices of HMs decreased in the order As (2.06) > Cu (2.00) > Pb (1.80) > Zn (1.72) > Ni (1.60) > Sb (1.39) > Cr (1.15) > Cd (1.07) > Mn (1.06) (Fig. S5). All mean single HM indices were > 1, indicating pervasive HM pollution and the impact of human activities. For HMs, 65.6% of Cr, 43.8% of Mn, 68.8% of Ni, 81.3% of Cu, 84.4% of Zn, 81.3% of As, 32.8% of Cd, 54.7% of Sb, and 59.4% of Pb were considered contaminated to different degrees, with As, Cu, Zn, and Pb being of particular concern.

This analysis demonstrates that PAH and HM contamination is prevalent in park soils. Most PAHs in karst park soils are derived from atmospheric deposition (Zhang et al. 2021), and HMs represent the superposition of background and atmospheric deposition (Han et al. 2022). Industries were previously the pillar of the Guiyang economy (Xu et al. 2016). Motor vehicle ownership has increased from 1.19 to 1.83 million, with increased petroleum PAH and HM emission (Stajic et al. 2016; Sun et al. 2021). Guiyang lies on the eastern Yunnan–Guizhou Plateau, and most parks are scattered over karst hill basins, which hinder the dispersion of atmospheric PAHs and HMs (Ma et al. 2020). Several other factors also enhance the deposition of atmospheric PAHs and HMs, including a low mean annual temperature (14.9 °C) and high precipitation frequency (236 d y^{-1}) and amount (1378 mm) (GSY 2021; Li et al. 2020), exacerbating the accumulation of PAHs and HMs in park soils. Management and control measures should therefore be undertaken to avoid further soil contamination.

Quantification of Potential Ecological Risks for Different Sources

The total TEQ of Σ_{16}PAH for different park soils ranged from 27.5 to 1979 (mean 110). Based on a safe BaP_{eq} value of 600 ng g^{-1} recommended by Canadian soil-quality guidelines (CCME 2010), the *TEQ* values of most park soils (98.4%) were below the safety limit. Nonetheless, the *TEQ* value for the TSGY park may be 3.3 times the 600 ng g^{-1} limit (Fig. S6), and higher than the World Health Organization standard value of 1000 ng g^{-1} (Qu et al. 2020). TSGY park is in Baiyun district, which was previously an industrial area (GSY 2021; Xu et al. 2016).

Toxic equivalent concentration values were lower than that reported in Lanzhou (mean 138 ng g^{-1}) (Jiang et al. 2016), Tianjin (124 ng g^{-1}) (Shi et al. 2021). Furthermore, *TEQ* values were strongly impacted by concentrations of DBA (58.0 ng g^{-1}), Bap (mean 31.7 ng g^{-1}), BaA (mean 6.34 ng g^{-1}), BkF (mean 5.65 ng g^{-1}), and BbF (mean 5.08 ng g^{-1}), contributing 52.7%, 28.8%, 5.76%, 5.14%, and 1.89%, respectively, and amounting to 97.1% of the total PAH concentration (Fig. S5b).

High *TEQ* values were distributed mainly in old urban areas (Baiyun and Yunyan districts) and former industrial areas (Baiyun district) (Fig. 3a). For old urban areas with rapid urbanization, long-term intensive anthropogenic activities may lead to elevated *TEQ* values in park soils. The PMF-based TEQ model indicates that PAH Factor 3 contributed to the generally high *TEQ* values in the study area. The contribution of Factor 3 (traffic sources) to TEQ was 49.9%, followed by biomass burning (20.5%), coal burning (18.0%), and coke oven (11.5%) (Fig. S7). The *TEQ* values of PAHs in urban park soils were thus most affected by traffic sources on the karst plateau, with contributions of individual PAHs being quite different from those of total Σ_{16}PAH.

The total *RI* value had a range of 27–647 (mean 141), indicating a low potential ecological risk (Table S6). The highest *RI* values were observed on the southern edge of Huaxi district (SLNC park), and the north-western edge of Baiyun district (YGSST) (Fig. 3f, Fig. S6), possibly as a result of industrial discharges (Xuan et al. 2018). E_i values of the nine HMs followed the order Sb > Cd > As > Cu > Pb > Ni > Cr > Zn > Mn (with all values other than that of Sb being < 40), indicating low ecological risk. Most HMs (100% of Cr, Cu, Mn, and Zn, 89.1% of As, 81.3% of Cd, and 98.4% of Pb) were categorized as low risk (Table S6 and Fig. S6). The maximum E_i values of Cd, Pb, and Sb were 190, 148, and 376, respectively, which are considered high, considerable, and extremely high risk levels, respectively.

HM Factor 2 was the predominant source of RI (Fig. S7). The results of PMF–RI modeling indicate that Factor 2 (coal burning) made the highest contribution to RI (41.7%), followed by Factor 1 (traffic sources, 27.5%), Factor 4 (natural sources, 19.1%), and Factor 3 (industrial sources, 11.7%). Effort in the monitoring and management of coal-burning and traffic sources is thus required to reduce the ecological risk posed by HMs in soil, although industrial sources should not be overlooked as re-emission may occur under certain conditions.

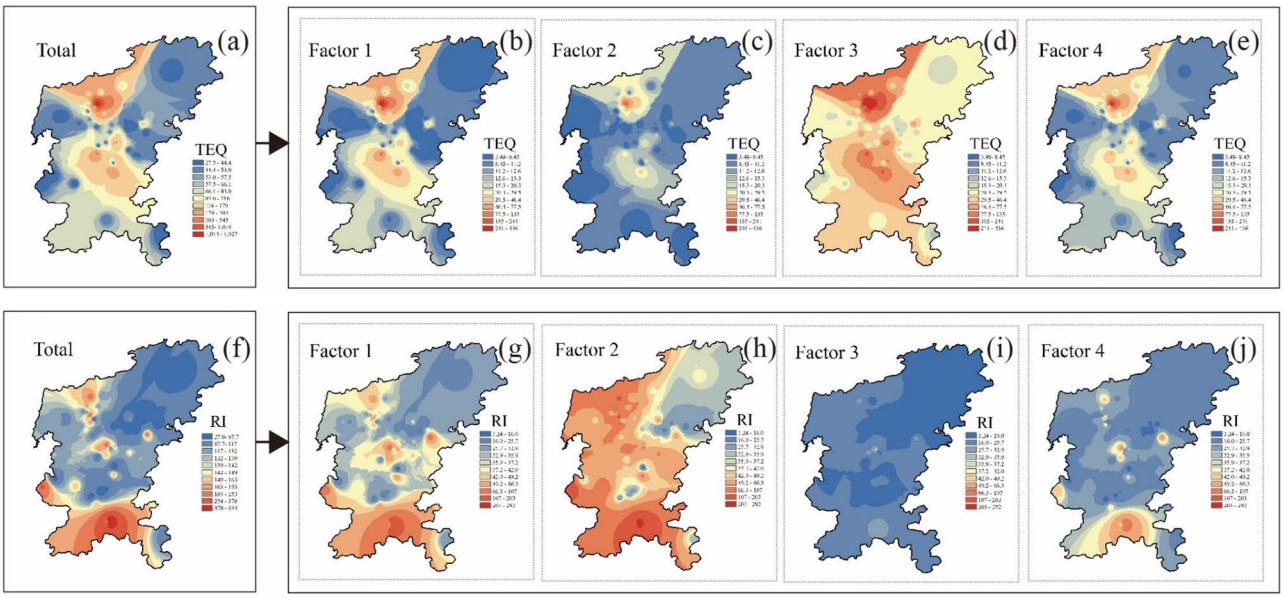

Fig. 3 Spatial distribution of PAH TEQs and total potential risk index (RI), and corresponding spatial distribution of associated source contributions. **a** total TEQ distribution of PAH, and **b–e** spatial contribution of different factors; **f** total RI distribution, and **g–j** spatial distribution of different factors

Human Health Risk of Different Sources

Human health risk evaluation is an effective tool for identifying toxic pollutants, exposure pathways, and pollution sources. To determine the human health risk caused by combinations of sources of PAHs and HMs, source-oriented human health risk was evaluated by MCs.

For both NCR and CR from PAHs and HMs, ingestion was the predominant exposure pathway (> 86.8%), followed by inhalation with a relatively minor contribution (Fig. S8). Ingestion of soil particles is thus the major exposure pathway for HMs in urban park soils on the karst plateau, and prevention is the key to risk reduction, as reported by previous studies (Huang et al. 2021; Liu et al. 2020).

With regard to NCR and TCR, children are exposed to higher PAH and HM levels than adults (Fig. 4). PAH HIs for children, male adults, and female adults were 3.47E–5, 3.84E–6, and 4.61E–6, respectively, at least four orders of magnitude lower than those of HMs (children mean 6.30E–1, male mean 8.05E–2; female mean 9.14E–2) (Fig. 4a, c). More attention should therefore be paid to HMs than PAHs in park soils to protect urban residents from high exposure risk. Among the HMs, As contributed most of the NCR and CR (Figs. S9, S10). Due to the elevated HMs levels recorded, their *HI* and *TCR* values were several times those of park soils in Shanghai, Beijing, Xiamen, Guangzhou (China), and Brno (Czech Republic) (Table 2).

The contributions of different factors contributing to human health risk were similar for all categories (children, female and male adults), regardless of their TCR and NCR (Fig. 5). PAH contributions to NCR followed the order biomass burning > traffic sources > coal burning > coke oven. However, for PAHs TCR, traffic sources contributed to 50%, followed by biomass burning, coal burning, and coke oven. The individual contributions of factors to health risk may be quite different from those of Σ_{16}PAH concentration, due to toxicity differences among PAHs.

For HMs, factors contributing to NCR and TCR were the same, with both following the order coal burning > natural sources > traffic sources > industrial sources (Fig. 6). Coal burning is thus the primary source of HM health risk, although the traffic sources and coal burning were the same sources of human health risk posed by PAHs and HMs together. The NCR and TCR of PAHs were several orders of magnitude lower than those of HMs, so the combined health risk is dominated by primary sources of HM risk. Coal burning plays a dominant role in health risk and HM concentrations and is a priority factor for the management and control of health risks posed by PAHs and HMs.

Human Health Risk and HM Bioavailability

As mentioned above, HMs contributed most to NCR and CR, so our further analysis focused only on health risks of HM fractions. Numerous studies have assessed HMs exposure risk based on total HM concentrations, however, their mobility and bioavailability vary. The sums of fractions 1, 2, and 3 were commonly considered as the bioavailable/potential bioavailable fractions, which may result in higher health risk relative to residual fractions (Zhao et al. 2020). No bioavailability assessment was undertaken in this study, the mobile and bioavailable fractions (1, 2, and fraction 3) were considered in evaluating health risk (Gope et al. 2017).

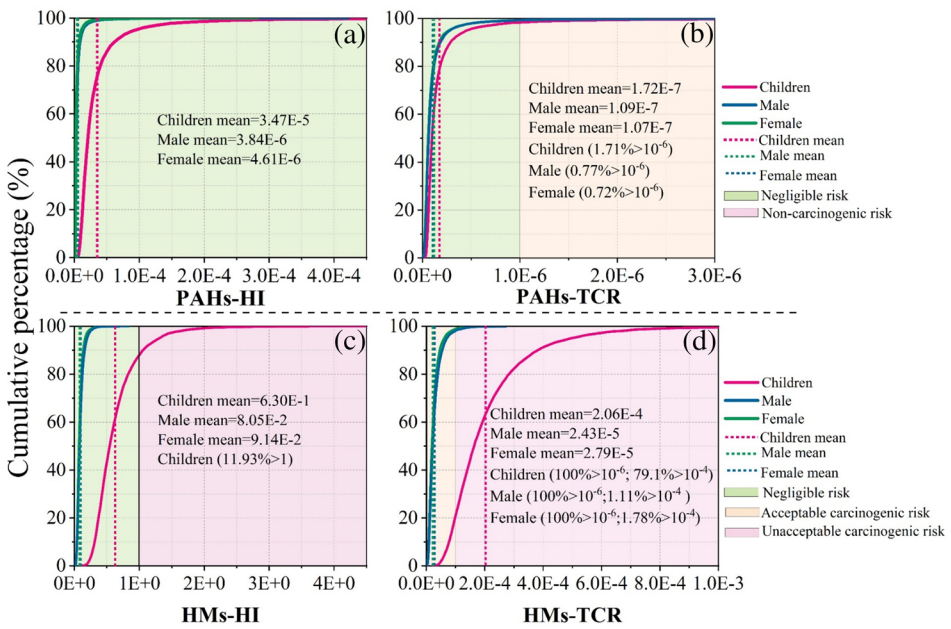

Fig. 4 Non-carcinogenic risk and total carcinogenic risk of PAHs and HMs

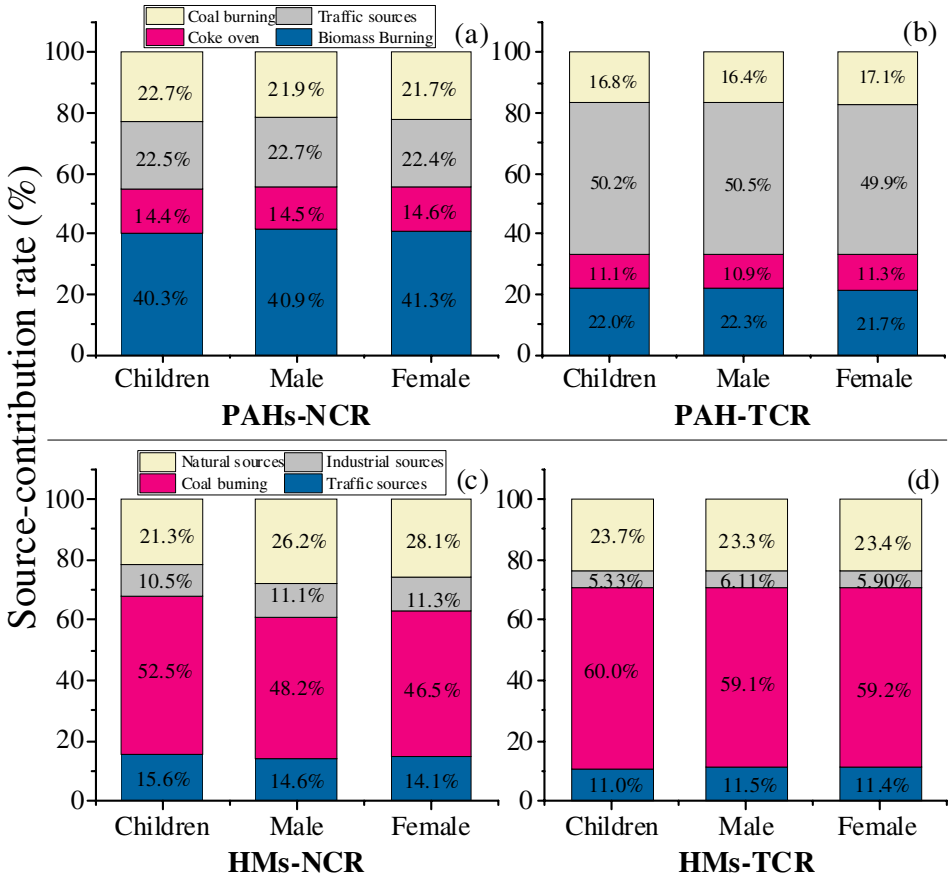

Fig. 5 Sources contribution rates corresponding to non-carcinogenic risk and carcinogenic risk of PAHs and HMs

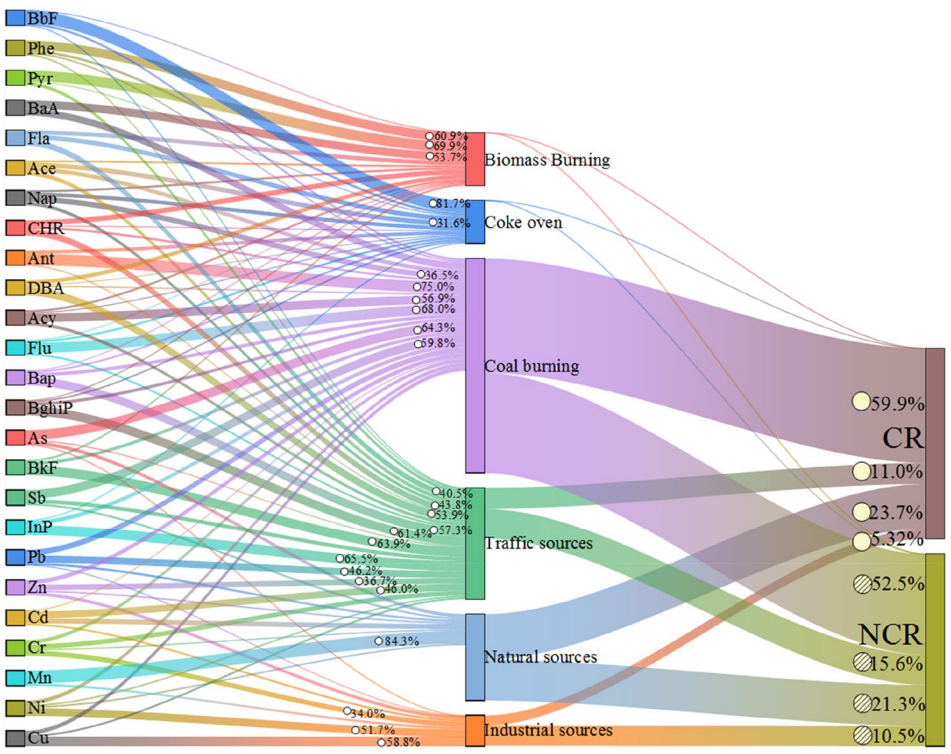

Fig. 6 Relationships among PAHs, HMs, joint pollution sources, and joint human health risk. Width of the curve indicates contribution rate

The concentrations of Ni, Cr, Cu, As, Sb, Zn, and Cd in park soils were generally dominated by Fraction 4 (residual) at 87.2%, 92.2%, 79.4%, 97.5%, 96.6%, 73.6%, and 42.3%, respectively. Lead had the highest Fraction 3 content (oxidizable, 36.8%), and Mn had a higher contribution of Fraction 2 (reducible, 55.6%). In contrast, the relatively mobile exchangeable Fraction 1 was generally low for all HMs Cd 17.7% > Mn 15.4% > Zn 3.97% > Ni 1.18% > Pb 1.14% > Sb 1.03% > Cu 0.382% > As 0.271% > Cr 0.0914%. For bioavailability (fractions 1 + 2 + 3), the order was Mn 78.5% > Pb 69.8% > Cd 57.7% > Zn 26.4% > Cu 20.6% > Ni 12.8% > Cr 7.83% > Sb 3.42% > As 2.51%.

In terms of HM bioavailability, the exposure levels were low for all HMs studied (Fig. 7), though children are exposed to higher health risk than adult females and males, regardless of HM bioavailability, likely due to the higher ratio of intake to body weight. Soil ingestion is also more prevalent among children (Wang et al. 2019b).

For NCR, the HIs for children, and adult males, and females were reduced to 11.0%, 18.3%, and 16.4%, respectively, of levels without consideration of bioavailability. When including bioavailability, the highest HQ shifted from As to Pb in all categories. With inclusion of bioavailability, *TCR* values for children, adult females, and adult males were 1.33E–5, 1.81E–6, and 1.57E–6, respectively, or ~ 6.50% of levels estimated without consideration of bioavailability; the highest *TCR* values were dominated by As and Mn.

With inclusion of bioavailability, Pb and Mn were thus identified as priority control pollutants. It is reassuring that, although total HM concentrations in park soils were higher on the karst plateau than other areas, the bioavailable fractions were generally lower than in other areas (Akoto et al. 2019), with correspondingly low exposure risk.

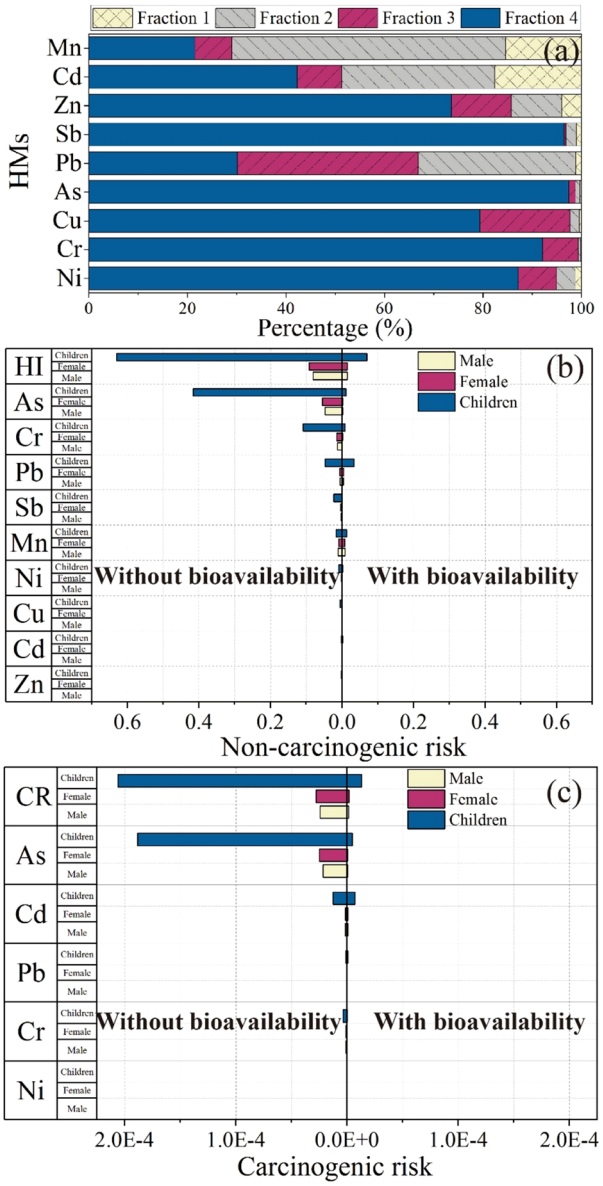

Fig. 7 Chemical speciation of HMs in urban park soils (**a**); non-carcinogenic risk with and without HM bioavailability (**b**); carcinogenic risk with and without HM bioavailability (**c**)

Global Implications of Priority Factors for Karst Urban Areas

The ecological environments of karst regions are fragile, and their ecosystems are threatened by natural and anthropogenic pressures. The high soil HM background is due mainly to soils associated with endogenous parent material and natural soil-forming processes in limestone areas, and to mining activities (Zhang & Wang 2020). The superposition of both natural and anthropogenic activities may pose higher potential health risks than those in non-karst areas. The global area of karst landscapes accounts for ~ 12% of global land areas, with such areas being distributed widely across the Mediterranean region, North Africa, South Asia, SW China, northern Australia, western North America, and southwestern South America (Yang et al. 2021). For urban areas experiencing rapid urbanization, soils in urban parks have experienced stresses associated with increasing populations and associated disturbances. Karst regions are also tourist attractions because of their unique scenery and ecosystems (Peng et al. 2017). The health risk due to soil contamination in urban karst areas is thus of special significance.

Conclusion

A study was undertaken of a typical karst plateau city, Guiyang, to determine the source-oriented ecological risks, and source-, pathway-, and speciation-oriented human health risks of PAHs and HMs in park soils. DBA and As were

the most concerning PAH and HM, respectively. Traffic sources and coal burning contributed most to the TEQ and RI, respectively. The NCR and TCR of HMs were several orders of magnitude higher than those of PAHs. Coal burning was the biggest contributor of NCR and TCR, and As was identified as a priority-pollutant. Ingestion is the primary exposure pathway for PAHs and HMs. Bioavailability of HMs contributes < 18.3 and 6.50% of NCR and TCR, respectively, based on total concentrations.

An integrated concept of priority control factors for the management of combined PAH and HM contamination of park soils in a karst high-background area is proposed. Control measures should include reduction in coal burning with a change to clean energy, increases in vegetation cover to reduce bare soil areas, and avoidance of soil ingestion by children.

Supplementary Information The online version contains supplementary material available at https://doi.org/10.1007/s12403-023-00534-3.

Acknowledgements This work was supported by National Natural Science Foundation of China (NSFC: 42003065), Guizhou science and technology supporting project Qiankehe [2020]1Y140, and China Postdoctoral Science Foundation (2019M663571).

Funding This study was funded by Young Scientists Fund, 42003065, Xiaohang Xu, Science and Technology Program of Guizhou Province, [2020]1Y140, Xiaohang Xu, Postdoctoral Research Foundation of China, 2019M663571, Xiaohang Xu.

Data availability The datasets generated and/ or analysed during this study are available from the corresponding author on reasonable request.

Declarations

Conflict of interest The authors declare that they have no known competing financial interests or personal relationships that could have appeared to influence the work reported in this paper.

References

Akoto O, Nimako C, Asante J, Bailey D, Bortey-Sam N (2019) Spatial distribution, exposure, and health risk assessment of bioavailable forms of heavy metals in surface soils from abandoned landfill sites in Kumasi, Ghana. Hum Ecol Risk Assess Int J 25(7):1870–1885. https://doi.org/10.1080/10807039.2018.1476125

Ambade B, Sethi SS, Chintalacheruvu MR (2022) Distribution, risk assessment, and source apportionment of polycyclic aromatic hydrocarbons (PAHs) using positive matrix factorization (PMF) in urban soils of East India. Environ Geochem Health. https://doi.org/10.1007/s10653-022-01223-x

Banger K, Toor GS, Chirenje T, Ma L (2010) Polycyclic Aromatic Hydrocarbons in urban soils of different land uses in Miami, Florida. Soil Sediment Contam: Int J 19(2):231–243. https://doi.org/10.1080/15320380903548516

Bao H, Hou S, Niu H, Tian K, Liu X, Wu F (2018) Status, sources, and risk assessment of polycyclic aromatic hydrocarbons in urban soils of Xi'an, China. Environ Sci Pollut Res 25(19):18947–18959. https://doi.org/10.1007/s11356-018-1928-z

Beane S, Comber S, Rieuwerts J, Long P (2016) Abandoned metal mines and their impact on receiving waters: a case study from Southwest England. Chemosphere 153:294–306. https://doi.org/10.1016/j.chemosphere.2016.03.022

Bineshpour M, Payandeh K, Nazarpour A, Sabzalipour S (2021) Status, source, human health risk assessment of potential toxic elements (PTEs), and Pb isotope characteristics in urban surface soil, case study: Arak city, Iran. Environ Geochem Health 43(12):4939–4958. https://doi.org/10.1007/s10653-020-00778-x

Brtnický M, Pecina V, Hladký J, Radziemska M, Koudelková Z, Klimánek M, Vaverková MD (2019) Assessment of phytotoxicity, environmental and health risks of historical urban park soils. Chemosphere 220:678–686. https://doi.org/10.1016/j.chemosphere.2018.12.188

Cai X, Zhao S, Wang J, Xuan B, Zhao S (2021) Vertical distribution features and risk assessment of heavy metals in arable soil surrounding an aluminum factory in Baiyun District of Guiyang. Environ Pollut Control 43(9):1183–1188. https://doi.org/10.15985/j.cnki.1001-3865.2021.09.018

CCME. (2010). (Canadian Council of Ministers of the Environment) polycyclic aromatic hydrocarbons. Canadian soil quality guidelines for protection of environmental and human health. Canadian soil quality guidelines. In: online available at: http://ceqgrcqe.ccme.ca/

Cetin B, Ozturk F, Keles M, Yurdakul S (2017) PAHs and PCBs in an Eastern Mediterranean megacity, Istanbul: their spatial and temporal distributions, air-soil exchange and toxicological effects. Environ Pollut 220:1322–1332. https://doi.org/10.1016/j.envpol.2016.11.002

Chen M, Huang P, Chen L (2013) Polycyclic aromatic hydrocarbons in soils from Urumqi, China: distribution, source contributions, and potential health risks. Environ Monit Assess 185(7):5639–5651. https://doi.org/10.1007/s10661-012-2973-6

Chen Z, Tian Z, Liu X, Sun W (2022) The potential risks and exposure of qinling giant pandas to polycyclic aromatic hydrocarbon (PAH) pollution. Environ Pollut. https://doi.org/10.1016/j.envpol.2021.118294

Chung M, Hu R, Cheung K, Wong M (2007) Pollutants in Hong Kong soils: polycyclic aromatic hydrocarbons. Chemosphere 67(3):464–473. https://doi.org/10.1016/j.chemosphere.2006.09.062

Ciarkowska K, Gambus F, Antonkiewicz J, Koliopoulos T (2019) Polycyclic aromatic hydrocarbon and heavy metal contents in the urban soils in southern Poland. Chemosphere 229:214–226. https://doi.org/10.1016/j.chemosphere.2019.04.209

Ciarkowska K, Konduracka E, Gambus F (2021) Primary soil contaminants and their risks, and their relationship to myocardial infarction susceptibility in Urban Krakow (Poland). Expo Health. https://doi.org/10.1007/s12403-021-00431-7

CNEMC (1990) (The Chinese Environmental Monitoring Centre) the background values of soil elements in China. China Environmental Science Press, Beijing

Cui H, Yang G, Cui W (2022) Distribution characteristics and risk assessment of soil heavy metal in karst peri-urban areas in Guanshan Lake district, Guiyang City. J Yunnan Agric Univ (Nat Sci) 37(2):173–179. https://doi.org/10.15985/j.cnki.1001-3865.2021.09.018

Dao L, Morrison L, Zhang H, Zhang C (2014) Influences of traffic on Pb, Cu and Zn concentrations in roadside soils of an urban park in Dublin, Ireland. Environ Geochem Health 36(3):333–343. https://doi.org/10.1007/s10653-013-9553-8

Edmondson JL, Davies ZG, McHugh N, Gaston KJ, Leake JR (2012) Organic carbon hidden in urban ecosystems. Sci Rep 2(1):963. https://doi.org/10.1038/srep00963

Fan X, Chen Z, Liang L, Qiu G (2019) Atmospheric PM2.5-bound polycyclic aromatic hydrocarbons (PAHs) in Guiyang City, Southwest China: concentration, seasonal variation, sources and health risk assessment. Arch Environ Contam Toxicol 76(1):102–113. https://doi.org/10.1007/s00244-018-0563-5

Gasiorek M, Kowalska J, Mazurek R, Pajak M (2017) Comprehensive assessment of heavy metal pollution in topsoil of historical urban park on an example of the Planty Park in Krakow (Poland). Chemosphere 179:148–158. https://doi.org/10.1016/j.chemosphere.2017.03.106

Gope M, Masto RE, George J, Hoque RR, Balachandran S (2017) Bioavailability and health risk of some potentially toxic elements (Cd, Cu, Pb and Zn) in street dust of Asansol, India. Ecotoxicol Environ Saf 138:231–241. https://doi.org/10.1016/j.ecoenv.2017.01.008

Greinert A (2015) The heterogeneity of urban soils in the light of their properties. J Soils Sediments 15(8):1725–1737. https://doi.org/10.1007/s11368-014-1054-6

GSY. (2021). Guiyang Statistical Yearbook. https://www.guiyang.gov.cn/zwgk/zfxxgks/fdzdgknr/tjxx/tjnj/

Gu Y, Li Q, Fang J, He B, Fu H, Tong Z (2014) Identification of heavy metal sources in the reclaimed farmland soils of the pearl river estuary in China using a multivariate geostatistical approach. Ecotoxicol Environ Saf 105:7–12. https://doi.org/10.1016/j.ecoenv.2014.04.003

Gu Y, Lin Q, Gao Y (2016) Metals in exposed-lawn soils from 18 urban parks and its human health implications in southern China's largest city, Guangzhou. J Clean Prod 115:122–129. https://doi.org/10.1016/j.jclepro.2015.12.031

Guan Q, Wang F, Xu C, Pan N, Lin J, Zhao R, Luo H (2018) Source apportionment of heavy metals in agricultural soil based on PMF: a case study in Hexi Corridor, northwest China. Chemosphere 193:189–197. https://doi.org/10.1016/j.chemosphere.2019.125272

Guan Q, Zhao R, Pan N, Wang F, Yang Y, Luo H (2019) Source apportionment of heavy metals in farmland soil of Wuwei, China: comparison of three receptor models. J Clean Prod 237:117792. https://doi.org/10.1016/j.jclepro.2019.117792

Hakanson L (1980) An ecological risk index for aquatic pollution control a sedimentological approach. Water Res 14(8):975–1001. https://doi.org/10.1016/0043-1354(80)90143-8

Han J, Liang L, Zhu Y, Xu X, Wang L, Shang L, Feng X (2022) Heavy metal(loid)s in farmland soils in the karst plateau, Southwest China–an integrated analysis of geochemical baselines, source apportionment and associated health risk. Land Degrad Dev 33(10):1689–1703. https://doi.org/10.1002/ldr.4257

Huang S, Liao Q, Hua M, Wu X, Bi K, Yan C, Zhang X (2007) Survey of heavy metal pollution and assessment of agricultural soil in Yangzhong district, Jiangsu Province, China. Chemosphere 67(11):2148–2155. https://doi.org/10.1016/j.chemosphere.2006.12.043

Huang J, Wu Y, Sun J, Li X, Geng X, Zhao M, Fan Z (2021) Health risk assessment of heavy metal(loid)s in park soils of the largest megacity in China by using Monte Carlo simulation coupled with positive matrix factorization model. J Hazard Mater. https://doi.org/10.1016/j.jhazmat.2021.125629

Huang C, Cai L, Xu Y, Wen H, Jie L, Hu G, Mei J (2022) Quantitative analysis of ecological risk and human health risk of potentially toxic elements in farmland soil based on PMF model. Land Degrad Dev 33(11):1954–1967. https://doi.org/10.1002/ldr.4277

Islam ARMT, Bodrud-Doza M, Rahman MS, Amin SB, Chu R, Al Mamun H (2019) Sources of trace elements identification in drinking water of Rangpur district, Bangladesh and their potential health risk following multivariate techniques and Monte-Carlo simulation. Groundwater Sustain Dev 9:100275. https://doi.org/10.1016/j.gsd.2019.100275

Izquierdo M, De Miguel E, Ortega MF, Mingot J (2015) Bioaccessibility of metals and human health risk assessment in community urban gardens. Chemosphere 135:312–318. https://doi.org/10.1016/j.chemosphere.2015.04.079

Jiang Y, Hu X, Yves UJ, Zhan H, Wu Y (2014) Status, source and health risk assessment of polycyclic aromatic hydrocarbons in street dust of an industrial city, NW China. Ecotoxicol Environ Saf 106:11–18. https://doi.org/10.1016/j.ecoenv.2014.04.031

Jiang Y, Yves UJ, Sun H, Hu X, Zhan H, Wu Y (2016) Distribution, compositional pattern and sources of polycyclic aromatic hydrocarbons in urban soils of an industrial city, Lanzhou, China. Ecotoxicol Environ Saf 126:154–162. https://doi.org/10.1016/j.ecoenv.2015.12.037

Jiang HH, Cai LM, Wen HH, Luo J (2020) Characterizing pollution and source identification of heavy metals in soils using geochemical baseline and PMF approach. Sci Rep 10(1):6460. https://doi.org/10.1038/s41598-020-63604-5

Jiang Y, Yuan L, Liang X, Nan Z, Deng X, Ma F (2021) Status, sources and potential risk of polycyclic aromatic hydrocarbons in soils from Hexi Corridor in Northwest China. Bull Environ Contam Toxicol. https://doi.org/10.1007/s00128-021-03312-6

Jiménez-Oyola S, Chavez E, García-Martínez M-J, Ortega M, Bolonio D, Guzmán-Martínez F, Romero P (2021) Probabilistic multipathway human health risk assessment due to heavy metal(loid)s in a traditional gold mining area in Ecuador. Ecotoxicol Environ Saf 224:112629. https://doi.org/10.1016/j.ecoenv.2021.112629

Jin Y, O'Connor D, Ok YS, Tsang DCW, Liu A, Hou D (2019) Assessment of sources of heavy metals in soil and dust at children's playgrounds in Beijing using GIS and multivariate statistical analysis. Environ Int 124:320–328. https://doi.org/10.1016/j.envint.2019.01.024

Katsoyiannis A, Terzi E, Cai Q (2007) On the use of PAH molecular diagnostic ratios in sewage sludge for the understanding of the PAH sources. Is this use appropriate? Chemosphere 69(8):1337–1339. https://doi.org/10.1016/j.chemosphere.2007.05.084

Ke C, Gu Y, Liu Q (2017) Polycyclic aromatic hydrocarbons (PAHs) in exposed-lawn soils from 28 urban parks in the Megacity Guangzhou: occurrence, sources, and human health implications. Arch Environ Contam Toxicol 72(4):496–504. https://doi.org/10.1007/s00244-017-0397-6

Khalili NR, Scheff PA, Holsen TM (1995) PAH source fingerprints for coke ovens, diesel and gasoline engines, highway tunnels, and wood combustion emissions. Atmos Environ 29(4):533–542. https://doi.org/10.1016/1352-2310(94)00275-P

Khan S, Munir S, Sajjad M, Li G (2016) Urban park soil contamination by potentially harmful elements and human health risk in Peshawar City, Khyber Pakhtunkhwa, Pakistan. J Geochem Explor 165:102–110. https://doi.org/10.1016/j.gexplo.2016.03.007

Kim KH, Jahan SA, Kabir E, Brown RJC (2013) A review of airborne polycyclic aromatic hydrocarbons (PAHs) and their human health effects. Environ Int 60:71–80. https://doi.org/10.1016/j.envint.2013.07.019

Kong J, Guo Q, Wei R, Strauss H, Zhu G, Li S, Zheng G (2018) Contamination of heavy metals and isotopic tracing of Pb in surface and profile soils in a polluted farmland from a typical karst area in southern China. Sci Total Environ. https://doi.org/10.1016/j.scitotenv.2018.05.034

Konstantinova E, Minkina T, Sushkova S, Antonenko E, Konstantinov A (2020) Levels, sources, and toxicity assessment of polycyclic aromatic hydrocarbons in urban topsoils of an intensively developing Western Siberian city. Environ Geochem Health 42(1):325–341. https://doi.org/10.1007/s10653-019-00357-9

Kwon H-O, Choi S-D (2014) Polycyclic aromatic hydrocarbons (PAHs) in soils from a multi-industrial city, South Korea. Sci

Total Environ 470–471:1494–1501. https://doi.org/10.1016/j.scitotenv.2013.08.031
Larsen RK, Baker JE (2003) Source apportionment of polycyclic aromatic hydrocarbons in the urban atmosphere: a comparison of three methods. Environ Sci Technol 37(9):1873–1881. https://doi.org/10.1021/es0206184
Lee CS-L, Li X, Shi W, Cheung SC-N, Thornton I (2006) Metal contamination in urban, suburban, and country park soils of Hong Kong: a study based on GIS and multivariate statistics. Sci Total Environ 356(1):45–61. https://doi.org/10.1016/j.scitotenv.2005.03.024
Li G, Sun G, Ren Y, Luo X, Zhu Y (2018) Urban soil and human health: a review. Eur J Soil Sci 69(1):196–215. https://doi.org/10.1111/ejss.12518
Li B, Zhou S, Wang T, Zhou Y, Ge L, Liao H (2020) Spatio-temporal distribution and influencing factors of atmospheric polycyclic aromatic hydrocarbons in the Yangtze River Delta. J Clean Prod 267:122049. https://doi.org/10.1016/j.jclepro.2020.122049
Li W, Wu J, Zhou C, Nsabimana A (2021) Groundwater pollution source identification and apportionment using PMF and PCA-APCS-MLR receptor models in Tongchuan City, China. Arch Environ Contam Toxicol 81(3):397–413. https://doi.org/10.1007/s00244-021-00877-5
Liang J, Feng CT, Zeng GM, Gao X, Zhong MZ, Li XD, Fang YL (2017) Spatial distribution and source identification of heavy metals in surface soils in a typical coal mine city, Lianyuan, China. Environ Pollut 225:681–690. https://doi.org/10.1016/j.envpol.2017.03.057
Liang J, Wu HB, Wang XX (2019) Distribution characteristics and health risk assessment of heavy metals and PAHs in the soils of green spaces in Shanghai, China. Environ Monit Assess 191(6):345. https://doi.org/10.1007/s10661-019-7476-2
Liu L, Liu Q, Ma J, Wu H, Qu Y, Gong Y, Zhou Y (2020) Heavy metal(loid)s in the topsoil of urban parks in Beijing, China: concentrations, potential sources, and risk assessment. Environ Pollut 260:114083. https://doi.org/10.1016/j.envpol.2020.114083
Liu Q, Wu Y, Zhou Y, Li X, Yang S, Chen Y, Ma J (2021) A novel method to analyze the spatial distribution and potential sources of pollutant combinations in the soil of Beijing urban parks*. Environ Pollut. https://doi.org/10.1016/j.envpol.2021.117191
Liu L, Wu J, He S, Wang L (2022) Occurrence and distribution of groundwater fluoride and manganese in the weining plain (China) and their probabilistic health risk quantification. Expo Health 14(2):263–279. https://doi.org/10.1007/s12403-021-00434-4
Liu L, Xu X, Han J, Zhu JM, Li S, Liang L, Wu P, Wu Q, Qiu G (2022) Heavy metal(loid)s in agricultural soils in the world's largest barium-mining area: Pollution characteristics source apportionment and health risks using PMF model and Cd isotopes. Proc Saf Environ Prot 166:669–681. https://doi.org/10.1016/j.psep.2022.08.061
Lu M, Yuan D, Ouyang T, Lin Q (2008) Source analysis and health risk assessment of polycyclic aromatic hydrocarbons in the topsoil of Xiamen Island. J Xiamen Univ 47(3):451–456. https://doi.org/10.1016/j.jclepro.2021.125833
Ma W, Zhu F, Liu L, Jia H, Yang M, Li Y (2020) PAHs in Chinese atmosphere part II: health risk assessment. Ecotoxicol Environ Saf 200:110774. https://doi.org/10.1016/j.ecoenv.2020.110774
Ma L, Li YH, Yao L, Du HM (2021) Polycyclic aromatic hydrocarbons in soil-turfgrass systems in urban Shanghai: contamination profiles, in situ bioconcentration and potential health risks. J Clean Prod. https://doi.org/10.1016/j.jclepro.2021.125833
Maliszewska-Kordybach B (1996) Polycyclic aromatic hydrocarbons in agricultural soils in Poland: preliminary proposals for criteria to evaluate the level of soil contamination. Appl Geochem 11(1):121–127. https://doi.org/10.1016/0883-2927(95)00076-3
Mallah MA, Li C, Mallah MA, Noreen S, Liu Y, Saeed M, Zhang Q (2022) Polycyclic aromatic hydrocarbon and its effects on human health: an overeview. Chemosphere 296:133948. https://doi.org/10.1016/j.chemosphere.2022.133948
Mostert MMR, Ayoko GA, Kokot S (2010) Application of chemometrics to analysis of soil pollutants. TrAC Trends Anal Chem 29(5):430–445. https://doi.org/10.1016/j.trac.2010.02.009
Paterson E, Sanka M, Clark L (1996) Urban soils as pollutant sinks —a case study from Aberdeen, Scotland. Appl Geochem 11(1):129–131. https://doi.org/10.1016/0883-2927(95)00081-X
Peng T, Deng H (2020) Comprehensive evaluation on water resource carrying capacity based on DPESBR framework: a case study in Guiyang, southwest China. J Clean Prod 268:122235. https://doi.org/10.1016/j.jclepro.2020.122235
Peng C, Ouyang Z, Wang M, Chen W, Li X, Crittenden J (2013) Assessing the combined risks of PAHs and metals in urban soils by urbanization indicators. Environ Pollut 178:426–432. https://doi.org/10.1016/j.envpol.2013.03.058
Peng X, Dai Q, Ding G, Zhu C, Li C (2017) Distribution and accumulation of trace elements in rhizosphere and non-rhizosphere soils on a karst plateau after vegetation restoration. Plant Soil 420(1–2):49–60. https://doi.org/10.1007/s11104-017-3363-1
Pies C, Hoffmann B, Petrowsky J, Yang Y, Ternes TA, Hofmann T (2008) Characterization and source identification of polycyclic aromatic hydrocarbons (PAHs) in river bank soils. Chemosphere 72(10):1594–1601. https://doi.org/10.1016/j.chemosphere.2008.04.021
Qu Y, Gong Y, Ma J, Wei H, Liu Q, Liu L, Chen Y (2020) Potential sources, influencing factors, and health risks of polycyclic aromatic hydrocarbons (PAHs) in the surface soil of urban parks in Beijing, China. Environ Pollut 260:114016. https://doi.org/10.1016/j.envpol.2020.114016
Ravindra K, Wauters E, Van Grieken R (2008) Variation in particulate PAHs levels and their relation with the transboundary movement of the air masses. Sci Total Environ 396(2):100–110. https://doi.org/10.1016/j.scitotenv.2008.02.018
Shi R, Li X, Yang Y, Fan Y, Zhao Z (2021) Contamination and human health risks of polycyclic aromatic hydrocarbons in surface soils from Tianjin coastal new region, China. Environ Pollut. https://doi.org/10.1016/j.envpol.2020.115938
Siemering G, Thiboldeaux R (2021) Background concentration, risk assessment and regulatory threshold development: polycyclic aromatic hydrocarbons (PAH) in Milwaukee, Wisconsin surface soils. Environ Pollut. https://doi.org/10.1016/j.envpol.2020.115772
Simcik MF, Eisenreich SJ, Lioy PJ (1999) Source apportionment and source/sink relationships of PAHs in the coastal atmosphere of Chicago and Lake Michigan. Atmos Environ 33(30):5071–5079. https://doi.org/10.1016/S1352-2310(99)00233-2
Solgi E, Oshvandi Z (2018) Spatial patterns, hotspot, and risk assessment of heavy metals in different land uses of urban soils (case study: Malayer city). Hum Ecol Risk Assess Int J 24(1):256–270. https://doi.org/10.1080/10807039.2017.1377597
Stajic J, Milenkovic B, Pucarevic M, Stojic N, Vasiljevic I, Nikezic D (2016) Exposure of school children to polycyclic aromatic hydrocarbons, heavy metals and radionuclides in the urban soil of Kragujevac city, Central Serbia. Chemosphere 146:68–74. https://doi.org/10.1016/j.chemosphere.2015.12.006
Sun X, Wang H, Guo Z, Lu P, Song F, Liu L, Wang F (2020) Positive matrix factorization on source apportionment for typical pollutants in different environmental media: a review. Environ Sci: Process Impacts 22(2):239–255. https://doi.org/10.1039/C9EM00529C
Sun Y, Tian Y, Xue Q, Jia B, Wei Y, Song D, Feng Y (2021) Source-specific risks of synchronous heavy metals and PAHs in inhalable particles at different pollution levels: variations and health

risks during heavy pollution. Environ Int. https://doi.org/10.1016/j.envint.2020.106162
Sun J, Zhao M, Huang J, Liu Y, Wu Y, Cai B, Fan Z (2022) Determination of priority control factors for the management of soil trace metal(loid)s based on source-oriented health risk assessment. J Hazard Mater. https://doi.org/10.1016/j.jhazmat.2021.127116
Tian H, Cheng K, Wang Y, Zhao D, Lu L, Jia W, Hao J (2012) Temporal and spatial variation characteristics of atmospheric emissions of Cd, Cr, and Pb from coal in China. Atmos Environ 50:157–163. https://doi.org/10.1016/j.atmosenv.2011.12.045
Tobiszewski M, Namieśnik J (2012) PAH diagnostic ratios for the identification of pollution emission sources. Environ Pollut 162:110–119. https://doi.org/10.1016/j.envpol.2011.10.025
Vega AS, Arce G, Rivera JI, Acevedo SE, Reyes-Paecke S, Bonilla CA, Pastén P (2022) A comparative study of soil metal concentrations in Chilean urban parks using four pollution indexes. Appl Geochem 141:105230. https://doi.org/10.1016/j.apgeochem.2022.105230
Wang W, Simonich S, Giri B, Chang Y, Zhang Y, Jia Y, Lu X (2011) Atmospheric concentrations and air–soil gas exchange of polycyclic aromatic hydrocarbons (PAHs) in remote, rural village and urban areas of Beijing-Tianjin region, North China. Sci Total Environ 409(15):2942–2950. https://doi.org/10.1016/j.scitotenv.2011.04.021
Wang C, Wu S, Zhou S, Wang H, Li B, Chen H, Shi Y (2015) Polycyclic aromatic hydrocarbons in soils from urban to rural areas in Nanjing: concentration, source, spatial distribution, and potential human health risk. Sci Total Environ 527–528:375–383. https://doi.org/10.1016/j.scitotenv.2015.05.025
Wang D, Luo P, Zou Z, Wang Q, Yao M, Yu C, Zhang A (2019) Alterations of arsenic levels in arsenicosis residents and awareness of its risk factors: a population-based 20-year follow-up study in a unique coal-borne arsenicosis county in Guizhou China. Environ Int 129:18–27. https://doi.org/10.1016/j.envint.2019.05.005
Wang M, Han Q, Gui C, Cao J, Liu Y, He X, He Y (2019) Differences in the risk assessment of soil heavy metals between newly built and original parks in Jiaozuo, Henan Province, China. Sci Total Environ 676:1–10. https://doi.org/10.1016/j.scitotenv.2019.03.396
Wang C, Wang J, Zhou S, Tang J, Jia Z, Ge L, Wu S (2020) Polycyclic aromatic hydrocarbons and heavy metals in urban environments: concentrations and joint risks in surface soils with diverse land uses. Land Degrad Dev 31(3):383–391. https://doi.org/10.1002/ldr.3456
Wang L, Li P, Duan R, He X (2022) Occurrence, controlling factors and health risks of Cr6+ in groundwater in the Guanzhong Basin of China. Expo Health 14(2):239–251. https://doi.org/10.1007/s12403-021-00410-y
Wei M, Wu J, Li W, Zhang Q, Su F, Wang Y (2022) Groundwater geochemistry and its impacts on groundwater arsenic enrichment, variation, and health risks in Yongning County, Yinchuan Plain of Northwest China. Expo Health 14(2):219–238. https://doi.org/10.1007/s12403-021-00391-y
Wu S, Zhou S, Bao H, Chen D, Wang C, Li B, Xu B (2019) Improving risk management by using the spatial interaction relationship of heavy metals and PAHs in urban soil. J Hazard Mater 364:108–116. https://doi.org/10.1016/j.jhazmat.2018.09.094
Xu X, Liu N, Landis MS, Feng X, Qiu G (2016) Characteristics and distributions of atmospheric mercury emitted from anthropogenic sources in Guiyang, southwestern China. Acta Geochim 35(3):240–250. https://doi.org/10.1007/s11631-016-0111-9
Xu X, Han J, Pang J, Wang X, Lin Y, Wang Y, Qiu G (2020) Methylmercury and inorganic mercury in Chinese commercial rice: implications for overestimated human exposure and health risk. Environ Pollut. https://doi.org/10.1016/j.envpol.2019.113706
Xuan B, Lu X, Wang J, Cai X, Duan Z, Hu F, Li D (2018) Spatial distribution characteristic and assessment of total and available heavy metals in karst periurban vegetable soil. IOP Conf Ser: Mater Sci Eng. https://doi.org/10.1088/1757-899X/392/4/042022
Yang B, Zhou L, Xue N, Li F, Li Y, Vogt RD, Liu B (2013) Source apportionment of polycyclic aromatic hydrocarbons in soils of Huanghuai Plain, China: comparison of three receptor models. Sci Total Environ 443:31–39. https://doi.org/10.1016/j.scitotenv.2012.10.094
Yang Q, Yang Z, Filippelli GM, Ji J, Ji W, Liu X, Zhang Q (2021) Distribution and secondary enrichment of heavy metal elements in karstic soils with high geochemical background in Guangxi, China. Chem Geol 567:120081. https://doi.org/10.1016/j.chemgeo.2021.120081
Yu H, Li T, Liu Y, Ma L (2019) Spatial distribution of polycyclic aromatic hydrocarbon contamination in urban soil of China. Chemosphere 230:498–509. https://doi.org/10.1016/j.chemosphere.2019.05.006
Yunker MB, Macdonald RW, Vingarzan R, Mitchell RH, Goyette D, Sylvestre S (2002) PAHs in the Fraser River basin: a critical appraisal of PAH ratios as indicators of PAH source and composition. Org Geochem 33(4):489–515. https://doi.org/10.1016/S0146-6380(02)00002-5
Zhan J, Li X, Christie P, Wu L (2021) A review of soil potentially toxic element contamination in typical karst regions in southwest China. Curr Opin Environ Sci Health 23:100284. https://doi.org/10.1016/j.coesh.2021.100284
Zhang Q, Wang C (2020) Natural and human factors affect the distribution of soil heavy metal pollution: a review. Water Air Soil Pollut 231(7):350. https://doi.org/10.1007/s11270-020-04728-2
Zhang Q, Yu R, Fu S, Wu Z, Chen H, Liu H (2019) Spatial heterogeneity of heavy metal contamination in soils and plants in Hefei, China. Sci Rep 9(1):1049. https://doi.org/10.1038/s41598-018-36582-y
Zhang Y, Peng C, Guo Z, Xiao X, Xiao R (2019) Polycyclic aromatic hydrocarbons in urban soils of China: distribution, influencing factors, health risk and regression prediction. Environ Pollut 254:112930. https://doi.org/10.1016/j.envpol.2019.07.098
Zhang Y, Chen H, Liu C, Chen R, Wang Y, Teng Y (2021) Developing an integrated framework for source apportionment and source-specific health risk assessment of PAHs in soils: application to a typical cold region in China. J Hazard Mater. https://doi.org/10.1016/j.jhazmat.2021.125730
Zhao LS, Hu GR, Yan Y, Yu RL, Cui JY, Wang XM, Yan Y (2019) Source apportionment of heavy metals in urban road dust in a continental city of eastern China: using Pb and Sr isotopes combined with multivariate statistical analysis. Atmos Environ 201:201–211. https://doi.org/10.1016/j.atmosenv.2018.12.050
Zhao L, Yan Y, Yu R, Hu G, Cheng Y, Huang H (2020) Source apportionment and health risks of the bioavailable and residual fractions of heavy metals in the park soils in a coastal city of China using a receptor model combined with Pb isotopes. Catena 194:104736. https://doi.org/10.1016/j.catena.2020.104736
Zheng H, Qu C, Zhang J, Talpur SA, Ding Y, Xing X, Qi S (2019) Polycyclic aromatic hydrocarbons (PAHs) in agricultural soils from Ningde, China: levels, sources, and human health risk assessment. Environ Geochem Health 41(2):907–919. https://doi.org/10.1007/s10653-018-0188-7
Zhou L, Dickinson RE, Tian Y, Fang J, Li Q, Kaufmann RK, Myneni RB (2004) Evidence for a significant urbanization effect on climate in China. Proc Natl Acad Sci USA 101(26):9540. https://doi.org/10.1073/pnas.0400357101
Zhuo HM, Wang X, Liu H, Fu SZ, Song H, Ren LJ (2020) Source analysis and risk assessment of heavy metals in development zones: a case study in Rizhao, China. Environ Geochem Health 42(1):135–146. https://doi.org/10.1007/s10653-019-00313-7